Dispersed Fluorescence and Computational Study of the 2 × 193 nm Photodissociation of $CHBr_3$ and CBr_4

Benjamin J. Petro, Eric D. Tweeten, and Robert W. Quandt*

Department of Chemistry, Illinois State University, Normal, Illinois 61790-4160

Received: July 9, 2003; In Final Form: September 18, 2003

The 2 × 193 nm photodissociations of $CHBr_3$ and CBr_4 have been examined using dispersed fluorescence. It was found that the initial photodissociation of $CHBr_3$ forms large amounts of $CH(A^2\Delta)$ while the photodissociation of CBr_4 forms lesser but still significant amounts of $CBr(A^2\Delta)$. Fluorescence rise time measurements show that photoproducts quickly react to form $C_2(d^3\Pi_g)$. In addition, the atomic and molecular bromine photoproduct channels were investigated using ab initio calculations. Intrinsic reaction coordinate calculations were performed at the MP2 level of theory using the LANL2DZ basis set to characterize the dissociation pathways for CBr_4 and $CHBr_3$. The results of the calculations show the presence of three transition states and an ion-pair isomer intermediate for both molecules. The broken symmetry structure of the transition states for the formation of molecular bromine is in agreement with the first step of the addition mechanism proposed by Cain and co-workers for $CX_2 + Y_2$ reactions.

I. Introduction

The photodissociation of halocarbons has received much interest due to the role these species play in stratospheric ozone depletion and as greenhouse gases.[1] In recent years bromine has received increased interest because it has a much greater potential for ozone destruction than chlorine.[2] Recent theoretical and experimental studies have shown that, in addition to better known sources such as Halons and methyl bromide, bromoform is a significant source of reactive bromine in the stratosphere.[3−5] Because of its obvious importance in stratospheric chemistry, several recent studies have looked at the photodissociation of bromoform at atmospherically important wavelengths. McGivern et al.[6] observed that at 193 nm the primary photoproduct was atomic bromine. They also observed secondary dissociation of the excited photoproduct, $CHBr_2$*, to form CBr and HBr. Xu et al.[7] observed the formation of atomic halogen in both the $^2P_{1/2}$ and $^2P_{3/2}$ spin states upon excitation at 234 and 267 nm. In addition, they found significant formation of molecular bromine with branching ratios into that channel of 0.16 and 0.26 at 267 and 234 nm, respectively.

While, as mentioned above, some work has been done on the photodissociation of $CHBr_3$, little work has been done on the photodissociation of CBr_4. The lone exception is an excimer photolysis study by Sam and Yardley.[8] In their work emission was observed from the $D' \rightarrow A'$ transition of molecular bromine, the 5p−5s transition from atomic bromine, and the $d^3\Pi_g \rightarrow a^3\Pi_u$ Swan bands of C_2 upon irradiation of CBr_4 with 2 × 249 nm photons. While they also obtained a photoproduct fluorescence spectrum from the 2 × 193 nm photodissociation of CBr_4, Sam and Yardley only discuss it in passing. They noted that, at 193 nm, the $Br(5p \rightarrow 5s)$ and $Br_2(D' \rightarrow A')$ emissions are absent. They speculate that while these species are most likely being formed, resonant transitions would be unlikely precluding fluorescence.

In this work we report on the 2 × 193 nm photodissociation of $CHBr_3$ and, for comparative purposes, CBr_4. In the dissociation of $CHBr_3$ we report, for the first time, the formation of a new reaction product, namely C_2. Both photodissociations were studied using both dispersed fluorescence and ab initio computational methods. In addition, the CBr_2 photoproduct from the photodissociation of CBr_4 was observed using cavity ringdown (CRD) absorption spectroscopy.

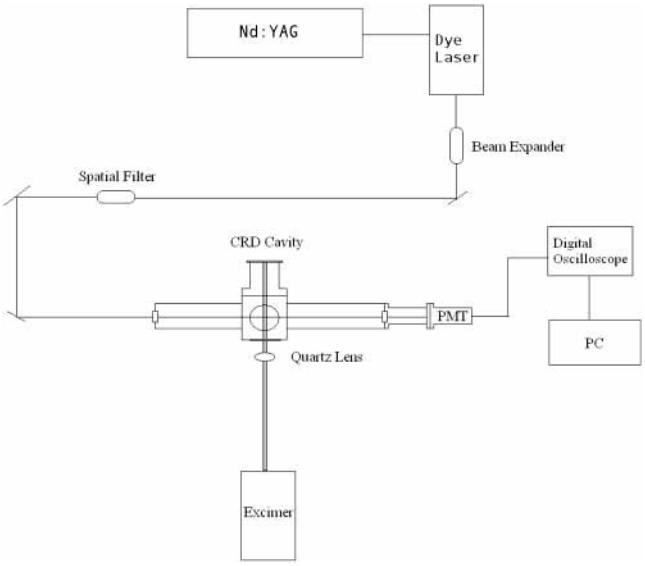

Figure 1. Diagram of the experimental apparatus.

II. Experimental Section

The experimental technique used consists of flowing ∼50 to 250 mTorr of $CHBr_3$ (Eastman) or CBr_4 (Aldrich Chemicals) through an 8 cm cubic cell, made of stainless steel, with five fused silica windows as shown in Figure 1. The back window of the cell was offset by an additional 8 cm with an aluminum tube to reduce scatter. The 193 nm photolysis source was an ArF excimer laser (Lambda Physik, Compex 110) operating at 10 Hz and 50−100 mJ. The excimer beam was focused into the cell with a quartz lens ($f = 100$ mm) with great care being

10.1021/jp035981r CCC: $27.50
Published on Web 12/24/2003

taken to ensure that the focal point was in the aluminum tube to prevent the absorption of three or more photons in the probe region. The absorption spectrum of CBr_2 was detected by crossing the photolysis beam, at right angles, with a Nd:YAG (Continuum Surelite I) pumped dye laser (Dakota Technology Inc.). Highly reflective mirrors ($R > 99.99\%$ at 630 nm) at the ends of each stainless steel arm form the ringdown cavity.

Extremely intense fluorescence signals were seen for both $CHBr_3$ and CBr_4 and were attributed to photoproduct emission. This fluorescence was collected at right angles to the excimer beam, with either a photomultiplier tube (Electron Tubes Limited Model 9129b) for the time and power dependence studies or a collimating lens coupled to a fiber optic cable for the dispersed fluorescence work. The fiber optic then transmitted the collected light to an asymmetric crossed Czerny−Turner monochromator (Ocean Optics Model S2000). An effective slit width of 8 μm and a 600 lines/mm grating give the monochromator a resolution of 1 nm. The dispersed light was detected with a CCD array, and the resulting signal was stored on a personal computer for later analysis. All chemicals were used without further purification and were stored in opaque containers, and in a freezer when not in use, to minimize photodegradation.

III. Computational Section

The Gaussian 98[9] electronic structure package was utilized on either a Linux-based personal computer or a Silicon Graphics O2 workstation for all calculations. To reduce the computational cost, all of the calculations employed the LANL2DZ basis, which consists of the Los Alamos effective core potential plus double-ζ valence-only basis for bromine.[10−12] For first-row atoms, the D95 double-ζ basis was used, leading to a basis consisting of 35 basis functions for $CHBr_3$ (41 for CBr_4).[13] Equilibrium geometries and transition-state structures were optimized at the MP2 level of theory and were verified by the calculation of vibrational frequencies. Convergence criteria for the geometry optimizations were that the root-mean-square gradient was less than or equal to 3×10^{-4} and the maximum component of the gradient was less than or equal to 1.2×10^{-3}. Single-point energies at the MP4 level of theory using the same basis set were then determined for the optimized structures. Neither the MP2 nor MP4 values were corrected for vibrational zero-point energies.

All transition states were confirmed by the presence of a single imaginary frequency in the vibrational analysis, and intrinsic reaction coordinate (IRC) calculations were run at the MP2 level of theory to verify that they corresponded to the correct reactants and products. In addition, a natural bond orbital (NBO) analysis[14] was carried out for all reactants, products, and transition states, once again at the MP2 level of theory, to determine the charge distribution using natural population analysis.[15,16]

IV. Results and Discussion

A. Power Dependence. Under excitation with focused 193 nm light, both $CHBr_3$ and CBr_4 exhibit strong UV and visible photoproduct fluorescence. Upon removal of the focusing lens, the fluorescence intensity is severely degraded but does not completely disappear. To determine the number of photons involved in the photodissociation, the photoproduct fluorescence intensity as a function of photolysis laser power was measured. A least-squares fit of the data gave power dependence values of 2.31 ± 0.46 for $CHBr_3$ and 1.60 ± 0.37 for CBr_4, indicating a two-photon process in each molecule. For the photodissociation of CBr_4, this is consistent with the results of Sam and Yardley,[8] who found that the fluorescence intensity went as the square of the photolysis power.

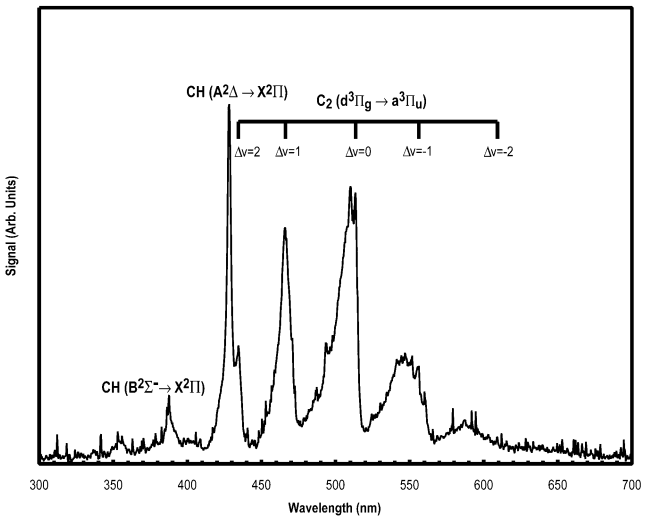

Figure 2. Dispersed emission spectra resulting from the 2 × 193 nm photodissociation of $CHBr_3$. The data shown are an average of several spectra and were corrected by subtracting an averaged background signal that was obtained in the absence of $CHBr_3$.

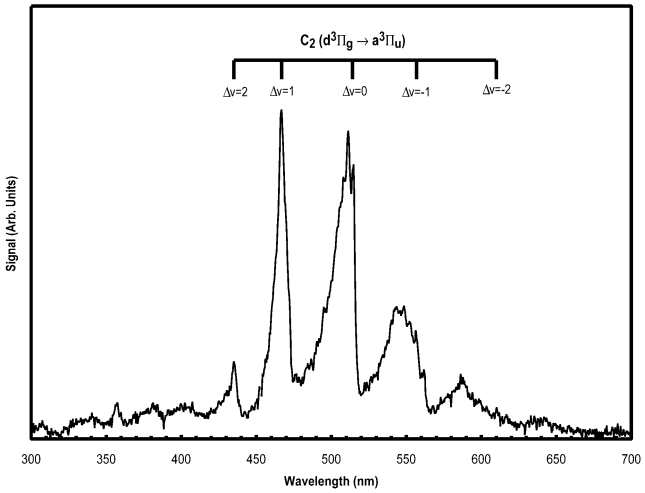

Figure 3. Dispersed emission spectra resulting from the 2 × 193 nm photodissociation of CBr_4. The data shown are an average of several spectra and were corrected by subtracting an averaged background signal that was obtained in the absence of CBr_4.

B. Photoproduct Spectra. The dispersed fluorescence spectra obtained by focusing the 193 nm excimer laser into samples of $CHBr_3$ and CBr_4 are shown in Figures 2 and 3, respectively.

Several of the common features of the fluorescence spectra are of interest. Both spectra contain bands with origins at 619, 563, 516, 473, and 438 nm which are degraded to the violet. These bands are assigned to the well-known Swan system ($d^3\Pi_g \rightarrow a^3\Pi_u$) of C_2.[17] As can be seen from the spectra, C_2 is formed with a moderate amount of vibrational excitation with two quanta of vibrational energy as is apparent in the $\Delta v = 0$ and $\Delta v = 2$ sequences. The former contains the $v' = 2 \rightarrow v'' = 2$ transition while the latter contains the $v' = 2 \rightarrow v'' = 0$ transition. The appearance of C_2 is somewhat puzzling due to the fact that the fluorescence rise time is detector limited (<30 ns) and appears after an induction period of approximately 100 ns. This is well under single collision conditions for this system (~600 ns/collision at 298 K for $CHBr_3$ or CBr_4), yet the formation is obviously a collisional process. A mechanism for its formation will be proposed below.

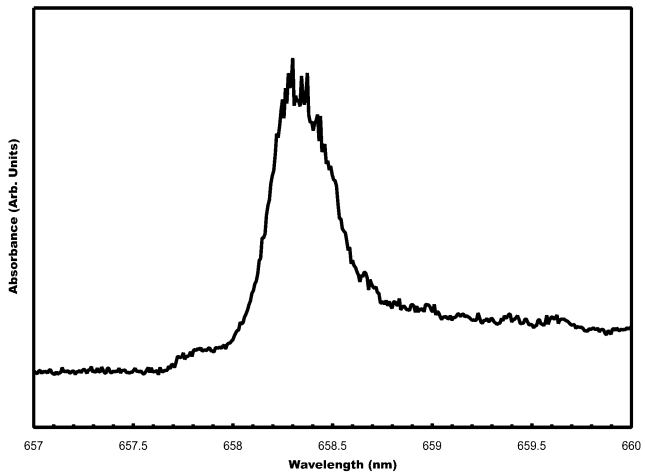

Figure 4. Cavity ringdown laser absorption of the photoproducts of the 2 × 193 nm photodissociation of CBr_4. Based on the work of Xu and Harmony,[18] the peak centered at 658.2 nm has been assigned to a combination of the $1_1^0 2_0^4$ hotband and 2_0^1 bending mode of the $\tilde{A}^1B_1 \leftarrow \tilde{X}^1A_1$ electronic transition of CBr_2.

Also of interest are the bands centered at 431 and 389 nm from the photolysis of $CHBr_3$. Both bands arise from the formation of excited-state CH. The former is the $A^2\Delta \rightarrow X^2\Pi$ transition, while the latter is the $B^2\Sigma^- \rightarrow X^2\Pi$ transition. Note that the analogous $A^2\Delta \rightarrow X^2\Pi$ transition of CBr was not observed in either this work or that of Sam and Yardley.[8] Finally, In agreement with the work of Sam and Yardley, emission from bromine atoms and molecules is absent in Figures 2 and 3.

Figure 4 shows the cavity ringdown (CRD) laser absorption spectrum of the photoproducts from the dissociation of CBr_4. Based on the work of Xu and Harmony,[18] the peak centered at 658.3 nm has been assigned to a combination of the $1_1^0 2_0^4$ hotband and 2_0^1 bending mode of the $\tilde{A}^1B_1 \leftarrow \tilde{X}^1A_1$ electronic transition of CBr_2. The resolution of the laser prevents separation of the individual bands. Because of interference from C_2 fluorescence, the exact induction time for the formation of CBr_2 could not be determined; however, it is ≤ 3 μs.

As stated above, the formation of C_2 (in under single collision conditions) and the lack of Br_2 and Br luminescence are somewhat puzzling. The apparent lack of Br and Br_2 fluorescence is much easier to explain and, therefore, will be discussed first. There is ample secondary evidence for the formation of both atomic and molecular bromine. First, in analogy with our previous work on CI_4 and CHI_3[19] as well as the work of Sam and Yardley at 249 nm,[8] and that of Xu et al.[7] at 234 and 267 nm, formation of the molecular product would be expected. Second, over the course of a run, there was a noticeable buildup of Br_2 in the cold trap of the vacuum pump. Third, initial scans, to detect CBr_2, of the CRD at ~620 nm would show a marked increase in absorbance after about 30 s. This absorption was broad, and at constant excimer power, the appearance time was constant. Increasing the photolysis power decreased the appearance time, indicating that the absorbance was due to the buildup of photoproduct in the cell. This absorbance was eventually assigned to the $Br_2(A^3\Pi_{1u} \leftarrow X^1\Sigma_g^+)$ absorption band. Finally, as mentioned above, the appearance of CBr_2 was fairly fast, indicating that it might be a primary photoproduct.

In their work on CBr_4 Sam and Yardley noted that at 248 nm there was enough energy to form Br_2 in the excited A′ state. Their argument is strengthened by ab initio calculations on CBr_4 and $CHBr_3$ in this work (which will be discussed below). These calculations show that at the transition state for the formation of CBr_2 and Br_2 the Br−Br bond length is 2.702 Å. This value is close to the experimental A′ state value of 2.68 Å. Once formed, the $Br_2(A')$ can absorb another 248 nm photon which in turn is followed by the observed D′ → A′ fluorescence. However, while there is more than enough energy available at 193 nm to form Br_2 in the A′ state, there is no analogous absorption to be followed by return fluorescence. Indeed, as was the case in this work, Sam and Yardley also noted that Br_2 fluorescence was absent in the 193 nm dissociation of CBr_4. Therefore, we conclude that a significant fraction of the photolysis forms Br and Br_2; however, under our experimental conditions it is not possible to observe either photoproduct.

The formation of $C_2(d^3\Pi_g)$ is more difficult to explain. Using simple collision theory, a 100 mTorr sample of pure CBr_4 at room temperature should have a collision approximately every 670 ns. However, as stated above, $C_2(d^3\Pi_g)$ fluorescence appears within 100 ns of the photolysis pulse, which is well under single collision conditions. In addition, 2 × 193 nm photons at 103 627 cm^{-1} would most likely not have enough energy to form C_2 from secondary reactions with the $CHBr_3$ or CBr_4 precursors. For example, using the heats of formation of Xu et al.,[7] the energy required to form C_2, that is, breaking seven C−Br bonds (eight for CBr_4) and one C−H bond, is ~200 000 cm^{-1}. Therefore, secondary reactions such as those shown in eqs 1−3 can be ruled out on energetic grounds because any intermediates would not be expected to have enough energy available to break the remaining C−H and C−Br bonds in order to form C_2.

$$CHBr_2 + CHBr_3 \rightarrow C_2 + \text{products} \quad (1)$$

$$CHBr + CHBr_3 \rightarrow C_2 + \text{products} \quad (2)$$

$$CH + CHBr_3 \rightarrow C_2 + \text{products} \quad (3)$$

Another possible source for the C_2 reaction product involves secondary reactions of photoproducts such as

$$CHBr_2 + CHBr_2 \rightarrow C_2 + \text{products} \quad (4)$$

$$CHBr + CHBr \rightarrow C_2 + \text{products} \quad (5)$$

$$CH + CH \rightarrow C_2 + H + H \quad (6)$$

$$CBr + CBr \rightarrow C_2 + Br + Br \quad (7)$$

However, reactions 4−7 would be expected to be extremely slow due to the low number densities typically associated with photoproducts.

A final possibility, as suggested by Sam and Yardley,[8] is the photodissociation of an impurity in the photolytic precursor. This scenario is unlikely for two reasons. First, the fluorescence of $C_2(d^3\Pi_g)$ in this study is striking for its intensity; it is easily observable with the naked eye. If it were being formed through a process involving an impurity, the fluorescence would be expected to be much weaker. Second, in addition to detecting $C_2(d^3\Pi_g)$ from $CHBr_3$ and CBr_4, preliminary work in our lab has detected fluorescence from $C_2(d^3\Pi_g)$ resulting from the photodissociation of CH_3CBr_3, CBr_3CH_2OH, and CCl_4. Since it is highly unlikely that all five precursors would have the same impurities (especially the CCl_4), the formation of $C_2(d^3\Pi_g)$ should be a primary process.

There are two important clues in the results that may give a possible mechanism for C_2 formation. The first is the CH peaks at 431 and 389 nm. Chen et al.[20] noted the formation of $CH(A^2\Delta)$ and $CH(B^2\Sigma^-)$ as primary photoproducts in the 3 ×

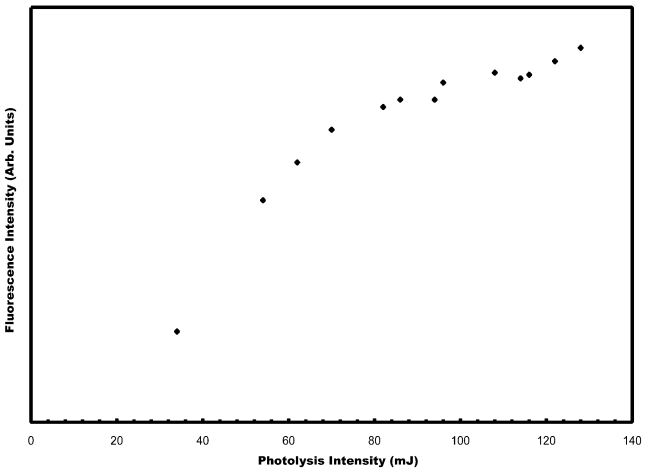

Figure 5. Power dependence data for the luminescence of $C_2(d^3\Pi_g)$ resulting from the 2 × 193 nm photodissociation of $CHBr_3$.

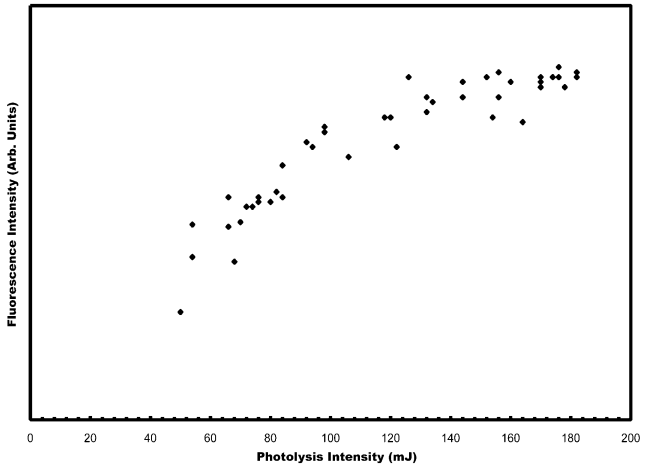

Figure 6. Power dependence data for the luminescence of $C_2(d^3\Pi_g)$ resulting from the 2 × 193 nm photodissociation of CBr_4.

266 nm photodissociation of $CHBr_3$. The sum of 3 × 266 nm photons is 112 782 cm^{-1}, which is only 9155 cm^{-1} more than the 103 627 cm^{-1} available in this work. Therefore, it seems likely that bromoform absorbs two 193 nm photons and either simultaneously or sequentially breaks all three carbon−bromine bonds. CBr_4 should exhibit similar behavior with the release of a CBr radical. Either case should be fast on the time scale of the experiment. However, even with the additional 25 707 cm^{-1} of electronic excitation in CH, radical processes such as reaction 3 would still occur in much longer than single collision times and be disallowed on energetic grounds. In addition, electronically excited CBr was not observed in this work or that of Sam and Yardley[8] in the 2 × 193 nm dissociation of CBr_4, indicating that the additional electronic energy is insufficient in and of itself to form C_2.

The second clue as to the origin of $C_2(d^3\Pi_g)$ in this system is the plots of fluorescence intensity versus excimer power for the photodissociation of both $CHBr_3$ and CBr_4 shown in Figures 5 and 6. As can be seen from the figures, even at moderate excimer powers (∼60−80 mJ) the photodissociation is saturated. This is due to the fact that both $CHBr_3$ and CBr_4 have significant absorbances at 193 nm, which provides a possible resonance enhancement for a two-photon absorption. Since experimental photolysis powers were in the range of 50−100 mJ, this means that under experimental conditions a significant fraction of the $CHBr_3$ or CBr_4 is undergoing photodissociation. It should also be noted that we were unable to observe the fluorescence threshold due to experimental constraints. If the $C_2(d^3\Pi_g)$ formation were due to reactions such as eqs 1−3, a linear power dependence would be expected in this region. However, as stated above these reactions are disallowed due to energetic considerations.

We therefore propose the following mechanism for the formation of electronically excited C_2 from the photodissociation of $CHBr_3$ and CBr_4.

Photolysis

$$CHBr_3 + 2h\nu(193\text{ nm}) \rightarrow CH(A^2\Delta) + 3Br + 7328\text{ cm}^{-1} \quad (8)$$

$$CBr_4 + 2h\nu(193\text{ nm}) \rightarrow CBr(A^2\Delta) + 3Br + 4334\text{ cm}^{-1} \quad (9)$$

Reaction

$CHBr_3$:

$$CH(X^2\Pi) + CH(X^2\Pi) \rightarrow C_2(a^3\Pi_u) + H + H - 7145\text{ cm}^{-1} \quad (10)$$

$$CH(A^2\Delta) + CH(X^2\Pi) \rightarrow C_2(a^3\Pi_u) + H + H + 16\,034\text{ cm}^{-1} \quad (11)$$

$$CH(A^2\Delta) + CH(A^2\Delta) \rightarrow C_2(a^3\Pi_u) + H + H + 39\,213\text{ cm}^{-1} \quad (12a)$$

$$\rightarrow C_2(d^3\Pi_g) + H + H + [16\,395(\Delta\nu = +2)\text{ to } 23\,061(\Delta\nu = -2)]\text{cm}^{-1} \quad (12b)$$

CBr_4:

$$CBr(X^2\Pi) + CBr(X^2\Pi) \rightarrow C_2(a^3\Pi_u) + Br + Br - 3406\text{ cm}^{-1} \quad (13)$$

$$CBr(A^2\Delta) + CBr(X^2\Pi) \rightarrow C_2(a^3\Pi_u) + Br + Br + 29\,356\text{ cm}^{-1} \quad (14a)$$

$$\rightarrow C_2(d^3\Pi_g) + Br + Br + [6538(\Delta\nu = +2)\text{ to } 13\,204(\Delta\nu = -2)\text{ cm}^{-1}] \quad (14b)$$

$$CBr(A^2\Delta) + CBr(A^2\Delta) \rightarrow C_2(a^3\Pi_u) + Br + Br + 62\,118\text{ cm}^{-1} \quad (15)$$

Note that the negative signs in reactions 10 and 13 indicate that they are endothermic. The photolysis steps, reactions 8 and 9, are proposed for several reasons. As discussed previously, the photodissociation of both species has been shown to be a two-photon process which adds 103 627 cm^{-1} to the system. A previous study by Chen et al.[20] found $CH(A^2\Delta)$ and $CH(B^2\Sigma^-)$ formation from $CHBr_3$ at similar excitation energies to this work. In addition, Seccombe et al.[21] have looked at the VUV photodissociation of CCl_3X (X = F, H, and Br). In their work they found that, due to a large density of states near the dissociation threshold, state-specific or isolated-state dissociation is less likely. This favors formation of the higher energy channel CX* + 3Cl as opposed to the lower energy production of Cl_2. Since $CHBr_3$ and CBr_4 have an even larger density of states, formation of CH* or CBr* would be expected to be even more probable than from CCl_3X. Finally, as can be seen in Figure 2,

large amounts of $CH(A^2\Delta)$ and even some $CH(B^2\Sigma^-)$ emission were directly detected from the photodissociation of $CHBr_3$.

The apparent lack of the analogous $CBr(A^2\Delta)$ emission from the photodissociation of CBr_4 is somewhat puzzling. As can be seen from reaction 9, there is more than enough energy to form it, and based on the work of Seccombe et al.[21] it would be the most likely channel. As can be seen from reaction 13, CBr ($X^2\Pi$) + CBr ($X^2\Pi$) does not have sufficient energy to form C_2 unless both CBr radicals have obtained an additional 3406 cm^{-1} of translation, rotational, and/or vibrational energy from the initial photodissociation. While this is quite possible, to form $C_2(d^3\Pi_g)$ an additional 19 360 cm^{-1} of energy is required, which is less likely. On the basis of secondary evidence, it appears that at least one electronically excited CBr is involved in the formation of C_2, yet as noted above, no CBr fluorescence was observed. This lack can be explained by several factors. First, the A state of CBr is ~9600 cm^{-1} higher in energy than the A state of CH, which puts its fluorescence in the 300−305 nm region. This is important because the sensitivity of the monochromator used in this experiment rapidly drops off in the UV region, reaching zero near 270 nm. This would severely attenuate any CBr fluorescence in this region. This problem is exacerbated by the general lack of sensitivity inherent in using a collimating lens and fiber optic to transmit light to the monochromator. Finally, and most importantly, $CBr(A^2\Delta)$ fluorescence is known to be diffuse due to predissociation of the $A^2\Delta_{3/2}$ state,[22] making it difficult to detect. We therefore conclude that at least some $CBr(A^2\Delta)$ is present although we cannot detect it.

Once formed, $CH(A^2\Delta)$ and $CBr(A^2\Delta)$ can react via processes such as reaction 3. However, since these processes are highly endothermic, most of these types of reactions can be excluded on energetic grounds. One possible exception that should be considered further is reaction 16, which is energetically allowed under experimental conditions.

$$CBr_2 + CBr(A^2\Delta) \rightarrow C_2(d^3\Pi_g) + Br + Br + Br + 5526\ cm^{-1} \quad (16)$$

In addition, the CRD absorption spectra show significant amounts of CBr_2 formation, giving both reactants relatively large concentrations. However, competing reactions such as eqs 12b and 14b are radical−radical reactions which would be expected to be barrierless, making them extremely fast. In addition, since reaction 16 is only exothermic by 5526 cm^{-1}, even a small barrier could prevent it from occurring. It should be noted that an attempt to calculate an activation energy for reaction 16 via an ab initio search for a transition state failed due to the high spin of the products. In addition, preliminary studies in this lab on the disappearance of CBr_2 show that the reaction is slow with a total rate constant on the order of 1×10^{-16} cm^3/(molecule s). Therefore, while we cannot definitively rule out this channel, it is expected to be minor at best.

Once formed, the $CH(A^2\Delta)$ or $CBr(A^2\Delta)$ molecules most likely proceed to form $C_2(d^3\Pi_g)$ through reactions 12b and 14b. These mechanisms are proposed for several reasons, some of which have been mentioned previously. The first is the photodissociation power dependences for $CHBr_3$ and CBr_4 which are shown in Figures 5 and 6, respectively. As can be seen from the figures, the absorbances of both molecules are saturated at moderate laser powers (80−100 mJ). Therefore, at the excimer energies used in this work a significant fraction of the precursors have undergone photodissociation. Second, the work of Seccombe et al.[21] and that of Chen et al.[20] show that a significant fraction of the photodissociation proceeds by forming CH* or, to a lesser extent, CBr*. Third, of the myriad of possible secondary reactions only reactions 12b and 14b (as well as reaction 15) are exothermic under experimental conditions. Finally, in order for reactions such as 10, 11, or 13 to form $C_2(d^3\Pi_g)$ the CH or CBr fragments would need a minimum of 25 000 cm^{-1} total, or 12 500 cm^{-1} per fragment, of translational, rotational, and vibrational energy. If the energy were divided equally, there would be approximately 4000 cm^{-1} of energy available in translation, rotation, and vibration. While this is certainly possible, all or a large fraction of the energy in each degree of freedom would then have to be converted into electronic energy in order to form the $C_2(d^3\Pi_g)$ product, which is highly unlikely. As stated above, the apparent lack of $CBr(A^2\Delta)$ fluorescence indicates that it is most likely being formed in smaller amounts than $CH(A^2\Delta)$. This is not a problem in that only one electronically excited CBr is necessary for formation of $C_2(d^3\Pi_g)$ (see reaction 14b), so even though there are smaller amounts of CBr to begin with, $C_2(d^3\Pi_g)$ fluorescence intensity from the $CHBr_3$ photodissociation is comparable to that from CBr_4.

C. Ab Initio Results. One photoproduct channel that is conspicuously absent in Figures 2 and 3 is the formation of molecular bromine. This is puzzling in that our previous work on CHI_3 and CI_4 detected large amounts of I_2* fluorescence under similar conditions.[19] In addition, in their work on the photodissociation of $CHBr_3$, Xu et al.[7] found a branching ratio of 0.26 into the Br_2 channel at 234 nm and 0.16 at 267 nm. Sam and Yardley[8] observed Br_2* emission at 248 nm, but noted it was absent at 193 nm. As discussed above, they also noted that $D' \rightarrow A'$ emission would be unlikely with irradiation at 193 nm.

To better understand this channel, and the photodissociation overall, ab initio calculations on the formation of the Br and Br_2 photoproducts were carried out. While the exact photodissociation mechanism is unknown, the work of Sam and Yardley combined with ab initio results from this work suggest that formation of Br_2 may occur on the ground-state surface. Similar calculations of ground-state mechanisms have proven useful in a study of the photodissociation of CHI_3 and CI_4.[19] To better follow this mechanism, an atom numbering system has been adopted and is shown in Figure 7. In general, the mechanism and structures are similar for both the CBr_4 and $CHBr_3$ dissociations. Therefore, unless otherwise specified, CBr_4 bond distances and angles will be used in the following discussion. Also, all the energetic results reported in this section are based on the MP4 single-point calculations obtained using the MP2-optimized geometries.

The calculated IRCs at the MP2 level for ground-state CBr_4 and $CHBr_3$ along with stable structures and transition-state structures are shown in Figures 8 and 9. Selected bond lengths, angles, and energies for these structures are given in Tables 1 and 2. The structures and energetic barriers shown in Figures 8 and 9 track remarkably well with the corresponding structures of Tweeten et al.[19] for the dissociation of CHI_3 and CI_4, with one exception that will be discussed shortly. For both molecules there are three primary transition states, hereafter referred to as TS1, molec. TS, and atomic TS, respectively. TS1 corresponds to a transition state from CBr_4 or $CHBr_3$ leading to formation of an ion-pair isomer of the parent molecule: either isobromomethane, CBr_3−Br, or isobromoform, $CHBr_2$−Br. The reaction path to this transition state involves Br5 migrating from its equilibrium position toward Br4. In the reactant the C2−Br5 distance is 2.040 Å and the Br4−Br5 distance is 3.331 Å. At

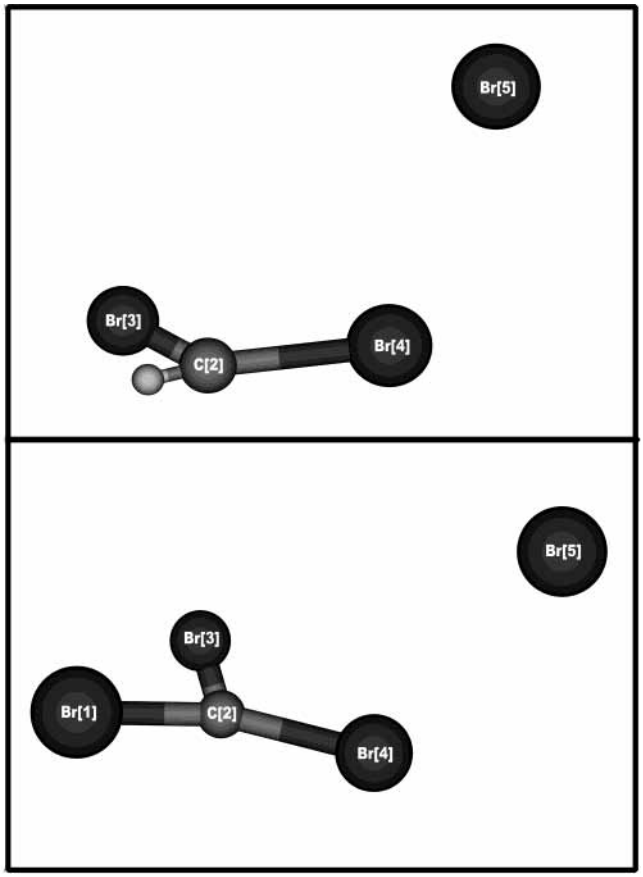

Figure 7. Schematic showing the atom numbering system used in the text for $CHBr_3$ (upper panel) and CBr_4 (lower panel). Both the $CHBr_3$ and CBr_4 structures shown are for the ion-pair isomer intermediates.

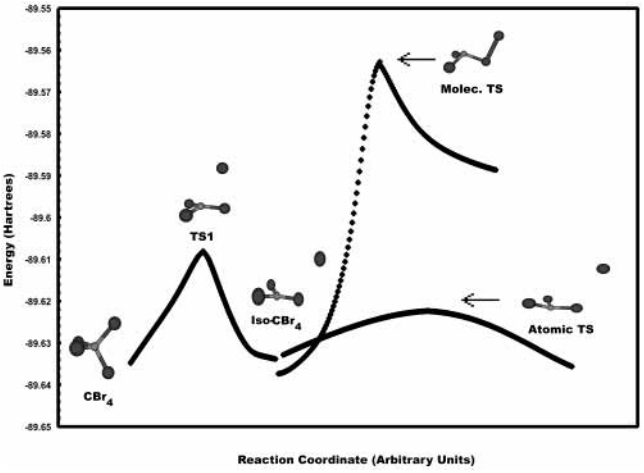

Figure 8. Calculated IRC for the ground-state dissociation of CBr_4 along with selected structures. All energies and structures shown were calculated at the MP2 level of theory with the LANL2DZ basis. The break in the IRC near the iso-CBr_4 structure is a computational artifact.

the TS1 structure these distances have changed to 3.328 and 3.158 Å, respectively. This step is followed by the CBr_3 moiety losing most of its pyramidal structure and becoming more planar. In $CHBr_3$ the Br3−C2−H1−Br4 dihedral angle changes by 53.28° to 173.28° at the transition state. In CBr_4 the change is less dramatic, but still significant, with the Br1−C2−Br3−Br4 angle changing by 39.05°.

Even on the ground-state surface significant charge transfer has already taken place when the system reaches TS1. The natural population analysis (NPA), summarized in Table 3,

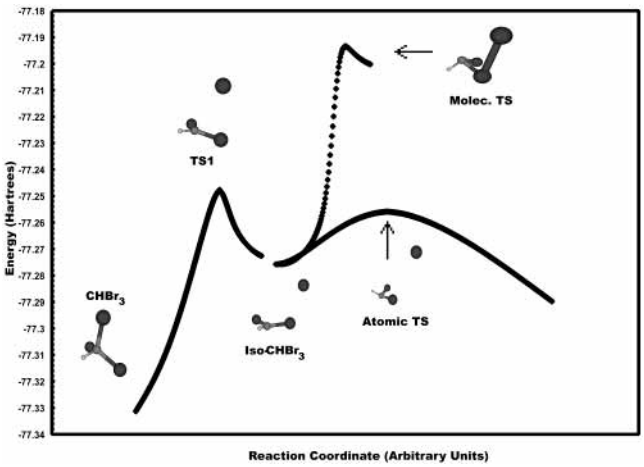

Figure 9. Calculated IRC for the ground-state dissociation of $CHBr_3$ along with selected structures. All energies and structures shown were calculated at the MP2 level of theory with the LANL2DZ basis. The break in the IRC near the iso-$CHBr_3$ structure is a computational artifact.

indicates that atom Br5 has gained 0.316 electron which is redistributed from the other three bromine atoms. The two bromine atoms that will form the carbene donate the least density, just 0.057. Atom Br4 loses the most electron density; its charge jumps from 0.158 to 0.380, a loss of 0.222 electron. $CHBr_3$ behaves in a similar manner with the exception that the charge differences are not as dramatic. This is not surprising since the hydrogen atom will be a poor donor of electron density compared to bromine. The energetic barrier to TS1, which is to formation of the ion-pair isomer, is 19 890 cm^{-1} for $CHBr_3$ and 16 464 cm^{-1} for CBr_4. In the actual experiment the initial excitation contains 83 737 cm^{-1} of energy above TS1 for $CHBr_3$ and 87 163 cm^{-1} for CBr_4. This means that an ion-pair state is most likely formed first, and then the bromine migration occurs.

As the dissociation proceeds from TS1, the CBr3 moiety passes through the planar structure and Br5 continues moving past Br4 until it reaches one of the ion-pair isomer intermediates (iso-$CHBr_3$ or iso-CBr_4) shown in Figure 7. At this point Br5 has moved outside of Br4 with the C2−Br5 distance increasing to 4.140 Å and the Br4−Br5 distance decreasing to 2.923 Å. The CBr_3 moiety has inverted with the Br1−C2−Br3−Br4 dihedral angle changing by an additional 44.09° to 156.86°. $CHBr_3$ also undergoes this inversion with a less dramatic change of angle. As would be expected, the charge separation is the largest for this structure. Br5 now has a natural charge of −0.230 while Br4 has increased to 0.417, a difference of 0.647 electron. This leads to stabilization of the iso-CBr_4 intermediate with the well depth from TS1 being 4484 cm^{-1}. The same well is 4728 cm^{-1} for iso-$CHBr_3$. The calculated well depth for iso-CBr_4 is somewhat surprising in that the same well for iso-CI_4 was found to be 523 cm^{-1}. This discrepancy can be explained, in part, by the difference in charge separation between I4 and I5 in ref 19 and Br4 and Br5 in this work. In the case of CI_4 the charge separation increases by 0.186 electron between the TS1 and iso-CI_4 structures. For CBr_4 the same structural change results in a more modest increase of 0.109 electron. This means that the iso-CI_4 structure should be higher in energy, relative to TS1, than the corresponding structures on the CBr_4 potential energy surface, reducing the well depth. For CHI_3 there is only a small increase, 0.049 electron, from TS1 to iso-CHI_3, resulting in a more stable structure with well depth of 7969 cm^{-1}. In the case of $CHBr_3$ the charge separation actually decreases by 0.026 electron, which results in a well depth of 4728 cm^{-1}. Note that,

TABLE 1: Selected Bond Distances (Å), Angles (deg), and Energies (au) for the Structures Shown in Figure 8[a]

parameter	CBr_4	CBr_4 TS1	iso-CBr_4	CBr_4 molec. TS	CBr_4 atomic TS	CBr_2 product
r(Br1−C2)	2.040	1.956	1.966	2.059	2.006	2.024
r(Br3−C2)	2.040	1.956	1.966	2.059	2.006	2.024
r(Br4−C2)	2.040	1.882	1.885	2.218	1.966	
r(Br5−C2)	2.040	3.328	4.140	3.414	5.154	
r(Br4−Br5)	3.331	3.158	2.923	2.702	3.952	
∠Br1−C2−Br3	109.47	117.65	117.51	111.43	114.57	111.15
∠C2−Br4−Br5	35.26	78.16	117.23	87.293	117.10	
∠Br1−C2−Br3−Br4	−120.00	−159.05	156.86	−121.12	134.67	
MP4 energy	−89.729 528	−89.654 510	−89.674 940	−89.607 504	−89.718 419	

[a] Geometric parameters are from the structures optimized at the MP2 level of theory using the LANL2DZ basis set. MP4 single-point energies were obtained using geometries optimized at the MP2 level.

TABLE 2: Selected Bond Distances (Å), Angles (deg), and Energies (au) for the Structures Shown in Figure 9[a]

parameter	$CHBr_3$	$CHBr_3$ TS1	iso-$CHBr_3$	$CHBr_3$ molec. TS	$CHBr_3$ atomic TS	HCBr product
r(H1−C2)	1.094	1.089	1.092	1.126	1.097	1.132
r(Br3−C2)	2.022	1.924	1.944	2.040	1.980	1.988
r(Br4−C2)	2.022	1.849	1.874	2.253	2.082	
r(Br5−C2)	2.022	3.275	4.088	3.522	5.200	
r(Br4−Br5)	3.349	3.104	2.893	2.601	3.541	
∠H1−C2−Br3	107.00	117.62	116.95	105.42	117.05	101.86
∠C2−Br4−Br5	34.09	78.31	116.46	92.76	133.58	
∠Br3−C2−H1−Br4	−120.00	−173.28	159.68	−112.35	−127.22	
MP4 energy	−77.379 596	−77.288 968	−77.310 511	−77.231 658	−77.359 200	

[a] Geometric parameters are from the structures optimized at the MP2 level of theory using the LANL2DZ basis set. MP4 single-point energies were obtained using geometries optimized at the MP2 level.

TABLE 3: Natural Population Analysis of Selected Equilibrium and Transition States on the CBr_4 and $CHBr_3$ Potential Energy Surfaces[a]

$CHBr_3$		CBr_4	
atom	natural charge	atom	natural charge
H(1)	0.240	C(2)	−0.634
C(2)	−0.559	Br(1)	0.158
Br(3)	0.106	Br(3)	0.158
Br(4)	0.106	Br(4)	0.158
Br(5)	0.106	Br(5)	0.158
$CHBr_3$ TS1		CBr_4 TS1	
atom	natural charge	atom	natural charge
H(1)	0.238	C(2)	−0.652
C(2)	−0.584	Br(1)	0.215
Br(3)	0.205	Br(3)	0.215
Br(4)	0.404	Br(4)	0.380
Br(5)	−0.262	Br(5)	−0.158
iso-$CHBr_3$		iso-CBr_4	
atom	natural charge	atom	natural charge
H(1)	0.224	C(2)	−0.575
C(2)	−0.525	Br(1)	0.194
Br(3)	0.151	Br(3)	0.194
Br(4)	0.395	Br(4)	0.417
Br(5)	−0.245	Br(5)	−0.230
$CHBr_3$ molec. TS		CBr_4 molec. TS	
atom	natural charge	atom	natural charge
H(1)	0.159	C(2)	−0.467
C(2)	−0.466	Br(1)	0.101
Br(3)	0.027	Br(3)	0.101
Br(4)	0.270	Br(4)	0.315
Br(5)	0.010	Br(5)	−0.050

[a] All calculations were obtained at the MP2 level of theory.

while not explicitly considered in the analysis above, steric effects most likely also play a significant role in the well depth. To refine the calculated energies and well depths, ab initio studies are currently underway using larger basis sets with added diffuse and polarization functions.

From the ion-pair states two different neutral product pathways are possible. The first is elimination of a bromine atom to form $CHBr_2$ + Br or CBr_3 + Br through the atomic TS. The structures of the atomic transition states shown in Figures 8 and 9 are by no means the only ones possible. Several transition structures with nearly the same energy were found for both $CHBr_3$ and CBr_4. Those shown in the figures were randomly chosen. It should be noted that in the IRC calculations shown in Figures 8 and 9 the energy actually drops below that of the free radical products. This is a computational artifact due to the dissociation from a singlet transition state to doublet products. High-level configuration interaction calculations would avoid this problem; however, such calculations are beyond the scope of this work.

The second pathway is the formation of molecular products. From the ion-pair isomers the reaction proceeds by elongation of the C2−Br4 bond while Br5 moves back toward C2. The CBr_3 moiety actually reinverts with the Br1−C2−Br3−Br4 dihedral angle changing by 87.97° to −112.35°. At the same time the Br4−Br5 distance decreases to 2.601 Å. Although this is longer than the ground-state Br_2 value of 2.281 Å, it is shorter than the D, D′, and E state equilibrium values, which are around 3.2 Å.[23−25] This indicates that no matter in which state Br_2 is formed it should have a large amount of vibrational excitation.

It should also be noted that while the IRCs in Figures 8 and 9 appear to be sharply peaked near the molec. TS they are, in fact, not. They only appear to be in comparison to the broad atomic transition states which compress the *x*-axis of Figures 8 and 9. This is demonstrated by the computed vibrational frequencies along the reaction path for CBr_4 and $CHBr_3$, which are 686i and 514i cm^{-1} for the molecular transition states and 84i and 70i cm^{-1} for the atomic transition states, respectively.

A key point is that in the structure of the molec. TS the C_{2v} subsymmetry present in CBr_4 has been broken, while for $CHBr_3$ this subsymmetry does not exist to be broken. This symmetry-broken structure was first proposed by Cain et al.[26] on the basis of frontier Hückel molecular orbital calculations. Their paper primarily focused on the addition reaction; however, their

arguments are still valid for the dissociation. The Hückel calculations showed the obvious insertion method, straightforward symmetric attack of the Br_2 by the carbene's sp^2 electrons, leads to a four-electron destabilization. This means that for CX_2Y_2 molecules any insertion pathway that keeps the C_{2v} symmetry is actually the highest in energy. The lower energy pathway is the nonsymmetric attack of the Lewis acidic p orbital on the central carbon of the carbene by a lone pair of the halogen. Their calculations predict an initial structure similar to the molec. TS structure shown in Figures 8 and 9. This is not surprising because in the reverse (dissociation) mechanism one would expect the final structure to be similar to the initial structure of the addition reaction.

The NPA also confirms the work of Cain et al.[26] As the dissociation proceeds from the ion-pair isomer, both C2 and Br5 lose charge. At the molec. TS C2 has lost 0.220 electron and Br5 has lost 0.239. Some of this loss is redistributed to Br1 and Br2 and the rest to Br4. However, the key point is that Br4 is still positively charged while C2 and Br5 are still negatively charged. This is not only in keeping with the work of Cain et al., but it shows that at the molec. TS, which is a late transition state, there is still significant charge separation (0.365) between Br4 and Br5. This suggests that Br_2 may be formed in an ion-pair state.

From the ion-pair isomer to the molec. TS there is an overall shift of 0.459 electron, which means that this transition state would be expected to be high in energy. For $CHBr_3$ the molec. TS is 17 306 cm^{-1} above the ion-pair isomer and 32 468 cm^{-1} above initial reactant. For CBr_4 it is 14 800 cm^{-1} above the ion-pair isomer and 26 781 cm^{-1} above the initial reactant.

The amount of excess energy available to the dissociating molecules depends on the photodissociation mechanism. In their work on CBr_4 Sam and Yardley proposed the following mechanism for dissociation at 248 nm:

$$CBr_4 + h\nu(248\ \text{nm}) \rightarrow CBr_2 + Br_2(A') \qquad (17)$$

$$Br_2(A') + h\nu(248\ \text{nm}) \rightarrow Br_2(D') \qquad (18)$$

This is then followed by $D' \rightarrow A'$ return fluorescence near 300 nm. If, as Sam and Yardley conjecture, reaction 17 occurs at 193 nm (51 813 cm^{-1}) as well, there would be 11 802 and 6115 cm^{-1} of excess energy available to CBr_4 and $CHBr_3$, respectively (assuming no excitation of the CBr_2 or CHBr photofragments). These relatively small numbers indicate that the ground-state surface could be important in the formation of molecular bromine. This is not surprising in that both CBr_4 and $CHBr_3$ should have a large density of states at 51 813 cm^{-1}. This would allow for effective internal conversion to lower energy states with large amounts of vibrational excitation. Another argument for the formation of Br_2 proceeding via a ground-state mechanism is that the computed Br4−Br5 bond distance at the molec. TS of CBr_4 is 2.702 Å, which is only 0.022 Å longer than the A′ state of Br_2. Formation of $Br_2(A')$ would be consistent with reaction 17.

V. Conclusions

The two-photon photodissociations of CBr_4 and $CHBr_3$ have been examined using both dispersed fluorescence and ab initio methods. Formation of electronically excited CH and CBr fragments from the initial photodissociation is followed by secondary radical−radical reactions which result in the formation of large amounts of $C_2(d^3\Pi_g)$.

The ab initio results show that the photodissociation proceeds first through a transition state to an ion-pair isomer. From this structure, the isomer can then dissociate into an atomic or molecular product channel with the molecular channel having the largest barrier. The calculated IRC pathway and the structure of the molecular and atomic transition states indicate that, while not directly observed, both molecular and atomic bromine photoproducts should be formed.

Acknowledgment. We thank both Dr. Joel Tellinghuisen and Dr. Robert Gordon for assistance in identifying and assigning the dispersed fluorescence spectra. We also thank Dr. Jean Standard for help with the ab initio calculations and for a critical review of this paper prior to publication. Acknowledgment is made to the Illinois State University Research Grant program for support of portions of this work.

References and Notes

(1) Molina, M. J.; Moline, L. T.; Kolb, C. E. *Annu. Rev. Phys. Chem.* **1996**, *47*, 327.

(2) Yung, Y. L.; Pinto, J. P.; Watson, R. J.; Sander, S. P. *J. Atmos. Sci.* **1980**, *37*, 339.

(3) Sturges, W. T.; Oram, D. E.; Carpenter, L. J.; Penkett, S. A.; Engle, A. *Geophys. Res. Lett.* **2000**, *27*, 2081.

(4) Dvortsov, V. L.; Geller, M. A.; Solomon, S.; Schauffler, S. M.; Atlas, E. L.; Blake, D. R *Geophys. Res. Lett.* **1999**, *26*, 1699.

(5) Barrie, L. A.; Bottenheim, J. W.; Schnell, R. C.; Crutzen, P. J.; Rasmussen, R. A. *Nature* **1998**, *334*, 138.

(6) McGivern, W. S.; Sorkhabi, O.; Suits, A. G.; Derecskei-Kovacs, A.; North, S. W. *J. Phys. Chem. A* **2000**, *104*, 10085.

(7) Xu, D.; Franscisco, J. S.; Huang, J.; Jackson, W. M. *J. Chem. Phys.* **2002**, *117*, 2578.

(8) Sam, C. L.; Yardley, J. T. *Chem. Phys. Lett.* **1979**, *61*, 509.

(9) Frisch, M. J.; Trucks, G. W.; Schlegel, H. B.; Scuseria, G. E.; Robb, M. A.; Cheeseman, J. R.; Zakrzewski, V. G.; Montgomery, J. A., Jr.; Stratmann, R. E.; Burant, J. C.; Dapprich, S.; Millam, J. M.; Daniels, A. D.; Kudin, K. N.; Strain, M. C.; Farkas, O.; Tomasi, J.; Barone, V.; Cossi, M.; Cammi, R.; Mennucci, B.; Pomelli, C.; Adamo, C.; Clifford, S.; Ochterski, J.; Petersson, G. A.; Ayala, P. Y.; Cui, Q.; Morokuma, K.; Malick, D. K.; Rabuck, A. D.; Raghavachari, K.; Foresman, J. B.; Cioslowski, J.; Ortiz, J. V.; Baboul, A. G.; Stefanov, B. B.; Liu, G.; Liashenko, A.; Piskorz, P.; Komaromi, I.; Gomperts, R.; Martin, R. L.; Fox, D. J.; Keith, T.; Al-Laham, M. A.; Peng, C. Y.; Nanayakkara, A.; Gonzalez, C.; Challacombe, M.; Gill, P. M. W.; Johnson, B. G.; Chen, W.; Wong, M. W.; Andres, J. L.; Gonzalez, C.; Head-Gordon, M.; Replogle, E. S.; Pople, J. A. *Gaussian 98*, revision A.7; Gaussian, Inc.: Pittsburgh, PA, 1998.

(10) Hay, P. J.; Wadt, W. R. *J. Chem. Phys.* **1985**, *82*, 270.

(11) Hay, P. J.; Wadt, W. R. *J. Chem. Phys.* **1985**, *82*, 284.

(12) Hay, P. J.; Wadt, W. R. *J. Chem. Phys.* **1985**, *82*, 299.

(13) Dunning, T. H., Jr.; Hay, P. J. *Modern Theoretical Chemistry*; Schaefer, H. F., III, Ed.; Plenum: New York, 1976; pp 1−28.

(14) Glendening, E. D.; Badenhoop, J. K.; Reed, A. E.; Carpenter, J. E.; Weinhold, F. *NBO 4.0*; Theoretical Chemistry Institute, University of Wisconsin: Madison, WI, 1996.

(15) Reed, A. E.; Weinhold, F. *J. Chem. Phys.* **1983**, *78*, 4066.

(16) Reed, A. E.; Weinstock, R. B.; Weinhold, F. *J. Chem. Phys.* **1985**, *83*, 735.

(17) Ballik, E. A.; Ramsay, D. A. *Astrophys. J.* **1963**, *137*, 61.

(18) Xu, S.; Harmony, M. D. *J. Phys. Chem.* **1993**, *97*, 7465.

(19) Tweeten, E. D.; Petro, B. J.; Quandt, R. W. *J. Phys. Chem. A* **2003**, *107*, 19.

(20) Chen, C.; Ran, Q.; Liu, S.; Yu, S.; Ma, X. *Huaxue Wuli Xuebao* **1993**, *6*, 299.

(21) Seccombe, D. P.; Tuckett, R. P.; Baumgärtel, H.; Jochims, H. W. *Phys. Chem. Chem. Phys.* **1999**, *1*, 773.

(22) Dixon, R. N.; Droto, H. W. *Trans. Faraday Soc.* **1963**, *59*, 1484.

(23) Sur, A.; Tellinghuisen, J. *J. Mol. Spectrosc.* **1981**, *88*, 323.

(24) Berwanger, P.; Viswanathan, K. S.; Tellinghuisen, J. *J. Mol. Spectrosc.* **1982**, *91*, 275.

(25) Van Marter, T. A.; Lu, Y.; Heaven, M. C.; Hwang, E.; Dagdigian, P. J.; Tellinghuisen, J. *J. Mol. Spectrosc.* **1996**, *177*, 311.

(26) Cain, S. R.; Hoffmann, R.; Grant, E. R. *J. Phys. Chem.* **1981**, *85*, 4046.